Risk Analysis, Vol. 26, No. 4, 2006 DOI: 10.1111/j.1539-6924.2006.00789.x

Physiologically-Based Pharmacokinetic Modeling of Benzene in Humans: A Bayesian Approach

Karen Yokley,[1] Hien T. Tran,[1] Kaija Pekari,[2] Stephen Rappaport,[3] Vesa Riihimaki,[4] Nat Rothman,[5] Suramya Waidyanatha,[3] and Paul M. Schlosser[6]*

Benzene is myelotoxic and leukemogenic in humans exposed at high doses (>1 ppm, more definitely above 10 ppm) for extended periods. However, leukemia risks at lower exposures are uncertain. Benzene occurs widely in the work environment and also indoor air, but mostly below 1 ppm, so assessing the leukemia risks at these low concentrations is important. Here, we describe a human physiologically-based pharmacokinetic (PBPK) model that quantifies tissue doses of benzene and its key metabolites, benzene oxide, phenol, and hydroquinone after inhalation and oral exposures. The model was integrated into a statistical framework that acknowledges sources of variation due to inherent intra- and interindividual variation, measurement error, and other data collection issues. A primary contribution of this work is the estimation of population distributions of key PBPK model parameters. We hypothesized that observed interindividual variability in the dosimetry of benzene and its metabolites resulted primarily from known or estimated variability in key metabolic parameters and that a statistical PBPK model that explicitly included variability in *only* those metabolic parameters would sufficiently describe the observed variability. We then identified parameter distributions for the PBPK model to characterize observed variability through the use of Markov chain Monte Carlo analysis applied to two data sets. The identified parameter distributions described most of the observed variability, but variability in physiological parameters such as organ weights may also be helpful to faithfully predict the observed human-population variability in benzene dosimetry.

KEY WORDS: Bayesian; benzene; dosimetry; human; metabolism; PBPK; variability

[1] Department of Mathematics and Center for Research in Scientific Computation, North Carolina State University, Raleigh, NC, USA.
[2] Biomonitoring Laboratory, Finnish Institute of Occupational Health, Helsinki, Finland.
[3] School of Public Health, University of North Carolina, Chapel Hill, NC, USA.
[4] Department of Occupational Hygiene and Toxicology, Finnish Institute of Occupational Health, Helsinki, Finland.
[5] Occupational and Environmental Epidemiology Branch, Division of Cancer Epidemiology and Genetics, National Cancer Institute, NIH, DHHS, Bethesda, MD, USA.
[6] CIIT Centers for Health Research, Research Triangle Park, NC, USA.
* Address correspondence to Paul M. Schlosser, U.S. EPA, NCEA, MD B243-01, RTP, NC, 27711; tel: 919-541-4130; fax: 919-685-3330; schlosser.paul@epa.gov.

1. INTRODUCTION

Benzene, a toxic industrial solvent, is a component of cigarette smoke and gasoline[1,2] and is also widely used in the production of many products. High-level exposure to benzene causes many health problems ranging from dizziness and headaches to anemia and leukemia.[3] A recent analysis of a prospective cohort study from the Australian petroleum industry showed an increased risk of leukemia. For the highest exposure group (>16 ppm-years) exposure intensity was strongly correlated with leukemia risk, with the increase starting around 0.8–1.6 ppm.[4] These toxic effects likely result from metabolites of benzene formed internally.[3,5] Therefore, studying

the mechanisms of benzene uptake, metabolism, and elimination through the body can assist in the assessment of acceptable levels of exposure.

Physiologically-based pharmacokinetic (PBPK) models are standard tools that are now often used in risk assessment to better extrapolate from experimental animals to humans and from high to low exposures; e.g., Haddad *et al.*,[6] Cahill *et al.*,[7] and Cole *et al.*[8] developed a PBPK model that predicts tissue concentrations of benzene and its key metabolites in mice using metabolic parameters obtained *in vitro*. The PBPK model's tissue compartments include the liver, richly perfused and poorly perfused tissues, and adipose tissue. Two additional compartments, the stomach and the alveolar gas-exchange region, were also included to describe oral and inhalation exposures, respectively. This model was later extended to take into account the zonal distribution of enzymes and metabolism in the liver, rather than treating the liver as one homogeneous compartment.[9,10] Most PBPK models have used single-valued parameters and hence are deterministic, though parameter distributions are increasingly being used to explicitly account for variability and uncertainty.

When PBPK models are extended to humans, accounting for the multiple sources of variability that affect dosimetry in humans is especially important. This hierarchy of variances includes population-wide variability, variability among different studies, differences between individuals within each study, and uncertainty in measurements taken from each individual. To properly account for the variability and uncertainty at any of these levels, PBPK models should be integrated into a statistical framework that acknowledges these sources of variation.

In classical pharmacokinetic analysis of data from drug trials, models with relatively simple structures and few empirical parameters are fit to data from a relatively large number of subjects, allowing for robust estimation of the distributions of those parameters. The fact that a volume of distribution, for example, would be estimated by fitting the model to the observed pharmacokinetic data is not considered a problem because the study population is assumed to be large and diverse enough to represent the ultimate target population for which predictions are desired. PBPK models have become popular in toxicology, however, because human dosimetry data are rare for environmental pollutants without therapeutic value. PBPK models overcome this data limitation because they make use of measured values for tissue compartments and blood flows (physiological parameters), which again are presumed to represent the larger population.

When a PBPK model fails to adequately fit pharmacokinetic data, however, one may consider varying the physiological parameters to fit the data, but updating population physiological parameters based on observations from a small sample could well result in posterior distributions not truly representative of the population as a whole. Tissue volumes and partition coefficients, for example, affect model predictions, and allowing them to vary can result in better model predictions than keeping them fixed, just as fitting the volume of distribution in classical pharmacokinetic models provides the flexibility to fit most data. One may question whether this flexibility results in a model that is more predictive of the population as a whole or whether it masks other errors in model specification. Because of these concerns and questions, analyses were performed keeping physiological parameters fixed while updating distributions for metabolic parameters, since prior information for metabolic parameters is much weaker and metabolic parameters are known to vary considerably among individuals.

In the current study, the Monte Carlo simulation program *MCSim*[11] was used to fit a PBPK model of benzene to sets of human data by performing a series of simulations along a Markov chain in the model parameter space. We hypothesized that the observed interindividual variability resulted primarily from known or estimated variability in key metabolic parameters and that a statistical PBPK model that explicitly included variability in *only* those metabolic parameters would be sufficient to describe all observed variability. Our objective was to test this hypothesis and ultimately identify parameter distributions for the PBPK model that would characterize the variability in the dosimetry of benzene and its key metabolites in humans.

2. METHODS

2.1. PBPK Model

The PBPK model used in this study is based on a previously developed PBPK model for benzene metabolism in mice.[9,10] Symbols and abbreviations used in the model are listed in Appendix 1. The system of ordinary differential equations derived from flow-limited assumption for tissue uptake is given in Appendix 2. To modify this model for risk assessment in humans, several parameters have to be adjusted.

Table I. Fixed Parameters Used in the PBPK Model[10]

Parameter	Value	Unit	Source
Q_L	$0.2370Q_{Card}$	L/hour	Davies and Morris[13]
Q_F	$0.0425Q_{Card}$	L/hour	Davies and Morris[13]
Q_K	$0.2027Q_{Card}$	L/hour	Davies and Morris[13]
Q_S	$0.1717Q_{Card}$	L/hour	Davies and Morris[13]
Q_R	$0.3461Q_{Card}$	L/hour	Davies and Morris[13]
V_L	$0.025BW$	L	Brown *et al.*[16]
V_F	$0.1429BW$	L	Davies and Morris[13]
V_K	$0.004BW$	L	Davies and Morris[13]
V_S	$0.734BW$	L	Brown *et al.*[16]
V_R	$0.040BW$	L	Brown *et al.*[16]
V_{Bl}	$0.07429BW$	L	Davies and Morris[13]
C^{CP}	14.5	mg/g	Csanady *et al.*[14]
C^{MP}	58	mg/g	Csanady *et al.*[14]
$K^{PH}_{m,1}$	1.4	μM	Seaton *et al.*[19]
$K^{PH}_{m,2}$	220	μM	Seaton *et al.*[19]
K^{HQ}_{m}	746	μM	Seaton *et al.*[19]
A^{BZ}	0.0397	1/μM	Lovern *et al.*[41]
A^{PH}	1.30×10^{-2}	1/μM	Lovern *et al.*[41]
A^{HQ}	10^{-7}	1/μM	Lovern *et al.*[41]
k_1	4.20×10^{-2}	L/μmol	Lovern *et al.*[41]
k_2	32.16	1/hour	Lovern *et al.*[41]
k_5	4.00×10^{-2}	L/μmol	Lovern *et al.*[41]
k_6	2.13×10^{-3}	L/μmol	Lovern *et al.*[41]
k_7	2.03×10^{-4}	L/μmol	Lovern *et al.*[41]
k_8	374.9598	1/hour	Cole *et al.*[10]
k_9	0.1163	1/hour	Cole *et al.*[10]
k_{10}	0.1443	1/hour	Cole *et al.*[10]

Table II. Partition Coefficients Used in the PBPK Model[10]

Parameter	Value	Source
$P^{BZ}_{Bl:Air}$	7.80	Brown *et al.*[37]
P^{BZ}_{F}, P^{BO}_{F}	54.50	Brown *et al.*[37]
P^{BZ}_{L}, P^{BO}_{L}	2.95	Brown *et al.*[37]
P^{BZ}_{S}, P^{BO}_{S}	2.05	Brown *et al.*[37]
P^{BZ}_{R}, P^{BO}_{R}, P^{BZ}_{K}, P^{BO}_{K}	1.92	Brown *et al.*[37]
P^{PH}_{F}	27.63	Leung *et al.*[42]
P^{PH}_{L}	2.17	Leung *et al.*[42]
P^{PH}_{S}	1.22	Leung *et al.*[42]
P^{PH}_{R}, P^{PH}_{K}	2.17	Leung *et al.*[42]
P^{HQ}_{F}	4.06	Leung *et al.*[42]
P^{HQ}_{L}	1.04	Leung *et al.*[42]
P^{HQ}_{S}	0.94	Leung *et al.*[42]
P^{HQ}_{R}, P^{HQ}_{K}	1.04	Leung *et al.*[42]

In particular, body weight (BW) was set at 70 kg for all individuals with the exception of the three individuals whose weights were recorded (Pekari *et al.*[12]; with personal correspondence). All fixed parameters used in the modified PBPK model can be found in Tables I and II. All blood flow rates and organ volumes were changed based on reference values for a 70-kg man. Physiological values from Davies and Morris[13] were calculated based on a reference weight of 70 kg and adjusted to satisfy the model requirement: $Q_{Card} = Q_F + Q_S + Q_R + Q_L + Q_K$. Partition coefficients ($P^{BZ}_{Bl:Air}$, P^{BZ}_{j}, and P^{BO}_{j} for compartments j = fat, liver, slowly perfused tissue, rapidly perfused tissue, and kidney) were also changed to adapt the model from mice to humans. The values for the concentration of microsomal protein per gram of tissue in the liver, C^{MP}, and the concentration of cytosolic protein per gram of tissue in the liver, C^{CP}, were changed from the original model and taken from Csanády *et al.*[14] A number of metabolic rate constants were assumed to be relatively invariant among species; hence, the remaining parameters in the PBPK model are unchanged from their values in Cole *et al.*[9,10]

The PBPK model also has equations describing the cumulative amount of exhaled benzene. To compare the model to data of the concentration of exhaled benzene, the following expression was used to compute the model value for concentration of benzene in exhaled air:

$$C^{BZ}_{E} = (1 - f_{alv}) \cdot C^{BZ}_{I} + f_{alv}\big[Q_{Card} \cdot (CV^{BZ} - CA^{BZ}) + Q_{AvV} \cdot C^{BZ}_{I}\big] \big/ Q_{AvV}. \quad (1)$$

The notation from the original model is preserved in Equation (1) with the only new value being f_{alv}, which is the fraction of each inhaled breath that perfuses the alveolar space. This equation is essentially identical to a correction used by Jonsson and Johanson[15] and is derived by assuming: air leaving the alveolar region satisfies the usual venous-equilibration model; air leaving the alveolar space mixes with air that was inhaled but only entered the physiological dead space (DS) in the conducting airways; the DS air does not exchange with blood at all and hence stays at the inhaled concentration; the measured exhaled concentration is the result of this mixture. Thus, the exhaled concentration equals f_{alv} times the concentration exiting the alveolar region plus $(1 - f_{alv})$ times the DS concentration that equals the inhaled concentration. The value for f_{alv} was set to be 0.67.[16] Additionally, the PBPK model has cumulative equations for urinary metabolites, and hence the model prediction

of the amount of urinary metabolite was divided by a standard value of urinary excretion as converted from 20 mL/kg/day to compute the predicted concentration over time.[17]

2.2. Statistical Analysis

To illustrate the statistical considerations, suppose that a multivariate PBPK model for benzene is specified by the n-dimensional system of differential equations:

$$\frac{dx}{dt} = f(t,\ x,\ q), \quad x(t=0) = x_0. \tag{2}$$

The solution to this system of equations denoted by $g(t,\ q,\ x_0)$ is a function of parameters q (including inhalation exposure conditions), time t, and initial condition x_0. Now, consider the case of *in vivo* data collected on each of m subjects exposed to benzene. Each of these subjects is assumed to follow the basic model (2), but with potentially different parameters and initial conditions, reflecting variation in pharmacokinetic parameters across the population. Although analysis of individual subject data provides insight into underlying biology, it fails to address the broader issue of how these parameters vary across individuals. Comprehensive application of PBPK models to these data requires that both levels of inquiry, individual and population, be addressed, not only to elucidate individual-specific parameter values but also to characterize the extent and nature of their variation across population.

Formally, for the ith individual, with intermittent observations available at time $t_{i1}, t_{i2}, \ldots, t_{in}$, let $Y_{ij} = (Y_{i1j}, Y_{i2j}, \ldots, Y_{imj})^T$ be the $(m \times 1)$ vector of observations on subject i at time t_{ij}; for example, Y_{ij} may include measurements of benzene in blood and expired air. Thus, data collected on individual i are the vectors $Y_{ij}, j = 1, 2, \ldots, n_i$, ideally assumed to be observations on the system (2). However, as mentioned earlier, the measurements of Y_{ij} are subject to several sources of variation. To specify this explicitly, we may specify the individual statistical model

$$Y_{ij} = g(t_{ij}, q_i, x_{0i}) + \varepsilon_{ij}, \quad j = 1, 2, \ldots, n_i, \tag{3}$$

where ε_{ij} is a random vector representing deviation of observed data from the dynamic model due to the combined effects of these sources at time t_{ij}, and q_i and x_{0i} are the parameters and initial conditions specific to individual i. Notice that the quantity of interest here is the distribution of parameters q_i.

The modified PBPK model was coded into Frédéric Bois' and Don Maszle's Monte Carlo simulation program, *MCSim* (version 5.0.0), which uses Metropolis-Hasting sampling for its MCMC simulations.[11] MCMC simulations were run on the model to find distributions of specific metabolic parameters that had been held constant in the previous PBPK modeling studies.[9,10] The model parameters investigated included V_{2E1}, the CYP2E1-specific activity as determined by the oxidation of *p*-nitrophenol to *p*-nitrocatechol; V_{PH1} and V_{PH2}, the maximum rates of metabolism of phenol by two sulphate transferases; and V_{HQ}, the maximum rate of conjugation for hydroquinone (primarily glucuronidation). The two first-order rates of metabolism of benzene oxide into phenylmercapturic acid (PMA) and muconic acid (MA), k_3 and k_4, respectively, were expected to vary within the population and hence were also updated according to the model and data through MCMC within the *MCSim* program. The result of Markov chain Monte Carlo (MCMC) fitting of the model to data produces samples from the Bayesian posterior distribution of the nine investigated model parameters.

The prior distributions for V_{2E1}, V_{PH1}, V_{PH2}, and V_{HQ} were determined by analyzing previous *in vitro* data obtained from human liver samples.[18] The initial rates of phenol sulfation and rates of hydroquinone glucuronidation from the *in vitro* study were each multiplied by factors given by the mathematical model used in Seaton *et al.*[19] The factors were 0.18 for V_{PH1}, 2.4 for V_{PH2}, and 11.1 for V_{HQ}. The CYP2E1 activity measurements were not multiplied by a factor. The distributions for these four parameters were assumed to be log-normal, and the means and standard deviations for the priors were set according to values computed from the data in Seaton *et al.*[18] Since little information was available on the other investigated parameters, the remaining priors were based on previous constant values. The prior distributions for k_3 and k_4 were also assumed to be log-normally distributed, and the (log-adjusted) means of these priors were computed from the fixed values from the original mouse model.[9,10] The standard deviations for k_3 and k_4 were set at 0.1 and 2 and then converted to log-space for implementation in the *Distrib* specification in *MCSim*. The *MCSim* program was used to find the distributional components for each of these model parameters, and the specific prior distributions used in the simulations are contained in Table III.

Data taken from previous studies of human benzene exposure were incorporated into the *MCSim* program, and extra specifications were used in the case of multiple data sets for the same individual to

Table III. Prior and Posterior Distributions for the PBPK Model Population Parameters Analyzed Using the Markov Chain Monte Carlo Method

Parameter	Prior Distribution	Posterior Distribution
k_3	Log-normal, $\mu = 0.70, \sigma = 0.10$	Log-normal, $\mu = 0.60, \sigma = 0.10$
k_4	Log-normal, $\mu = 15.0, \sigma = 2.0$	Log-normal, $\mu = 12.1, \sigma = 1.69$
V_{2E1}	Log-normal, $\mu = 0.0782, \sigma = 0.0511$	Log-normal, $\mu = 0.012, \sigma = 0.013$
V_{PH1}	Log-normal, $\mu = 0.0302, \sigma = 0.0118$	Log-normal, $\mu = 0.038, \sigma = 0.032$
V_{PH2}	Log-normal, $\mu = 0.4029, \sigma = 0.1577$	Log-normal, $\mu = 0.48, \sigma = 0.38$
V_{HQ}	Log-normal, $\mu = 0.7484, \sigma = 0.3207$	Log-normal, $\mu = 1.05, \sigma = 1.05$

find interindividual variability as opposed to intraindividual variability. In one study, blood and exhaled air samples were collected from three healthy nonsmokers who were each exposed to 4-hour periods of both 10 cm^3/m^3 and 1.7 cm^3/m^3 benzene.[12] Thirty-five occupationally exposed individuals provided urine samples during their work shifts for metabolite data in a second study.[20,21] Even though the time length of their shifts and urine collection times varied, the exposure time for these workers was taken to be 6 hours in the model. The MCMC simulation was run for 20,000 iterations, and the results were recorded every 10th iteration. The results were analyzed from iteration 15,010 through 20,000 to ascertain the distributions of the model parameters.

2.3. Sensitivity Analysis

After the posterior distributions were determined, the model was examined for sensitivity. The means of each posterior distribution were used for the investigated parameters to produce solutions from the model. To ascertain the sensitivity of the model to each parameter, one parameter was varied while all the other investigated parameters were kept at the mean values from their posterior distributions. For each investigated parameter, three solutions were produced, respectively, using the parameter mean decreased by 1%, the mean of the currently analyzed parameter, and the mean of the parameter increased by 1%. The solutions were computed for a time period of 0 to 10 hours so that the length of that time range could be searched for the greatest value of sensitivity. Although sensitivity coefficients are often computed by choosing a time point and then evaluating the sensitivity there, finding a maximum difference in solutions over a range of time gives a more thorough estimate of the maximum sensitivity of each parameter.[22] After the magnitude of the maximum distance (i.e., the absolute value of the maximum difference) between the mean solution and the solution above or below the mean curve was computed, it was used in the following formula to evaluate sensitivity:

$$Sensitivity = \frac{\Delta Prediction/Prediction}{\Delta Parameter/Parameter}.$$

In the above formula, $\Delta prediction$ indicates the maximum distance between the predicted solution using the mean parameter value and the predicted solution using the mean value increased or decreased by 1%, and *prediction* indicates the predicted solution using the mean parameter value at the time when that maximum difference occurs. The mean was chosen as the basis for comparison in the sensitivity analysis simply because it is a measure of central tendency and was not chosen in particular because of any statistical reasoning. The values in the denominator of the above ratio are based on the varying investigated parameter and are defined similar to the predicted solutions. The only state variables of the model examined for sensitivity were those compared to data in this study in addition to the product of phenol and hydroquinone blood concentrations.

2.4. Covariance Analysis

Covariance matrices were computed from the *MCSim* output in order to ascertain whether any investigated parameters were correlated. Output values from 15,010 through 20,000 for the population mean of each investigated parameter (not corrected from the log-space *MCSim* output) were used to compute one covariance matrix, and covariance matrices were computed for the values produced (again, iteration 15,010 through 20,000) for each of the three individuals from Pekari *et al.*[12]

3. RESULTS

Originally, the *MCSim* program was run five times with five different seeds for its random number

generator. The distributions resulting from these five runs were analyzed, and the output for the model parameters V_{PH1} and V_{PH2} did not have any well-fitting parametric distributions. The output for V_{2E1} varied greatly among the five runs; specifically, three of the runs yielded much higher V_{2E1} output distributions than the other two. Additionally, even when simulations were run using selective subsets of the output distributions (i.e., fitting distributions to only two or three chosen outputs of the five based on the magnitude of the V_{2E1} output), the resulting model solution distributions were very narrow. After changing the priors to be log-normally distributed, the *MCSim* program was run again. A single long run was assumed to be sufficient as suggested in Geyer,[23] although Bois and Maszle believe that integrating several pooled runs is a better approach.[11]

The output from *MCSim* appeared to sample adequately from the posterior distributions, and the posterior distributions for the six investigated model parameters are shown in Table III as well as compared graphically to their priors in Fig. 1. The individual distributions for the three subjects from Pekari *et al.*[12] are contained in Table IV. As shown in Fig. 1, the posterior population distribution for k_3 shifted slightly to the left of its prior. The posterior distributions for k_4 and V_{PH2} moved left as well but more significantly than k_3 and also narrowed relative to their priors. The posterior distributions for the metabolic rates V_{PH1} and V_{HQ} broaden somewhat but otherwise do not greatly differ from values from *in vitro* data.[19] The posterior distribution for V_{2E1} narrowed considerably around the left-most portion of the prior.

A set of 100 samples was selected randomly from the posterior distribution of the set of six investigated parameters for each of the three individuals in Pekari *et al.*[12] (Matlab's uniform random number function was used to make the selection from the posterior distributions independently. Since the covariance analysis discussed later indicates little correlation between variables, this independent sampling seems reasonable. The array of six parameter values randomly selected was then taken as the sample.) An implementation of the model code in Matlab was then used to simulate the time course for exhaled air and blood benzene (at high and low exposure levels) for each of these 100 samples for each individual, and the results plotted against the original data in Figs. 2–5 (cloud of black points). Here, the solution curves are plotted for each individual in the study to determine whether the data points (symbols) fall in the area created by the range of the solutions. The solutions for the three individuals are plotted separately because their model solutions depended on different body weights (90 kg for Subject 1, 55 kg for Subject 2, and 73 kg for Subject 3). A final set of 100 random parameter-vector samples was likewise chosen from the posterior distribution for the population mean parameters (other than body weights, for which individual values were still used), and simulation results with those parameters are also included in Figs. 2–5 (cloud of gray points). As one might expect, the range of solutions obtained using

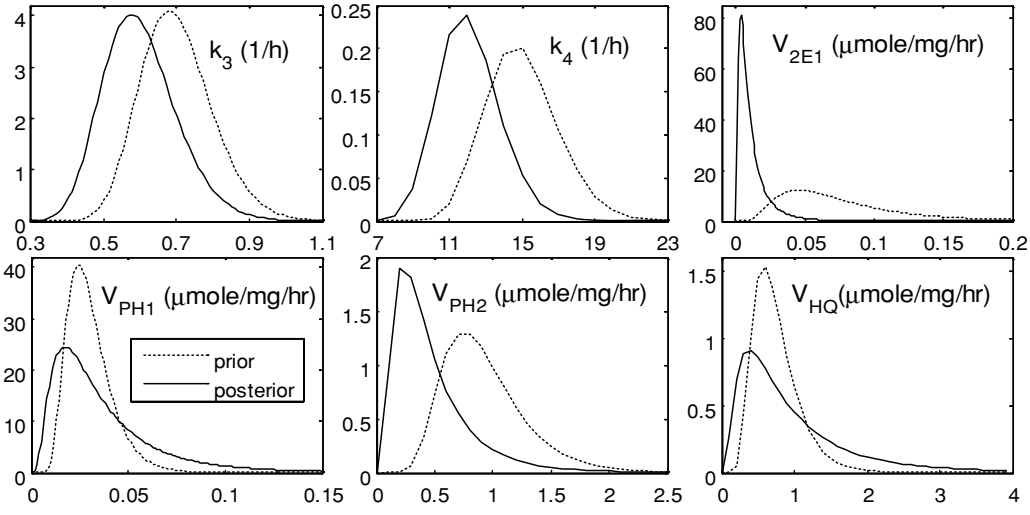

Fig. 1. Prior and posterior distributions for the six investigated parameters.

Table IV. Posterior Individual Parameter Distributions for the Three Subjects of Pekari *et al.*[12]

Parameter	Log-Normal Distribution (Subject 1)	Log-Normal Distribution (Subject 2)	Log-Normal Distribution (Subject 3)
k_3	$\mu = 0.605, \sigma = 0.150$	$\mu = 0.597, \sigma = 0.148$	$\mu = 0.613, \sigma = 0.153$
k_4	$\mu = 12.2, \sigma = 2.82$	$\mu = 12.2, \sigma = 2.87$	$\mu = 12.4, \sigma = 3.13$
V_{2E1}	$\mu = 0.0503, \sigma = 0.0125$	$\mu = 0.239, \sigma = 0.0926$	$\mu = 0.166, \sigma = 0.0681$
V_{PH1}	$\mu = 0.0460, \sigma = 0.0562$	$\mu = 0.0453, \sigma = 0.0465$	$\mu = 0.0409, \sigma = 0.0375$
V_{PH2}	$\mu = 0.508, \sigma = 0.479$	$\mu = 0.552, \sigma = 0.638$	$\mu = 0.535, \sigma = 0.505$
V_{HQ}	$\mu = 1.19, \sigma = 1.41$	$\mu = 1.13, \sigma = 1.07$	$\mu = 1.28, \sigma = 1.35$

the sample from the individual posterior distributions was much narrower than that obtained with the overall population distribution.

As with the analysis of the model with the data from Pekari *et al.*,[12] 100 samples were drawn from the posterior distribution found through *MCSim* for the occupational exposure[20,21] and a corresponding set of simulations (using the measured exposure concentration for that individual) was obtained using Matlab. The resulting 100 simulated values for each urinary metabolite were then plotted in Fig. 6 against the corresponding measured values. So each vertical line of *x*s in Fig. 6 represents the 100 model-simulated urinary metabolite concentrations for a given exposure, plotted with the x-value set to the measured concentration. A plot of the line $y = x$ is contained in all parts of Fig. 6 for comparison, and again the results are plotted on both linear and log-scale to ascertain the models performance at both lower and higher concentrations. All five metabolite solutions were somewhat centered around the $y = x$ line except for the plots of the catechol and trihydroxy benzene concentration and the hydroquinone conjugate concentration. However, the predictions for both catechol/trihydroxy benzene concentration and hydroquinone conjugate concentration do better match the low concentration, as shown in the log-scale plots.

The results of the sensitivity analysis are listed in Table V. The values in the table are based on the ratio of prediction change over parameter change as listed in Section 2 and are all nonnegative because they are absolute value of the highest sensitivity in the model in the interval 0–10 hour. The columns represent the parameter being changed and rows represent the

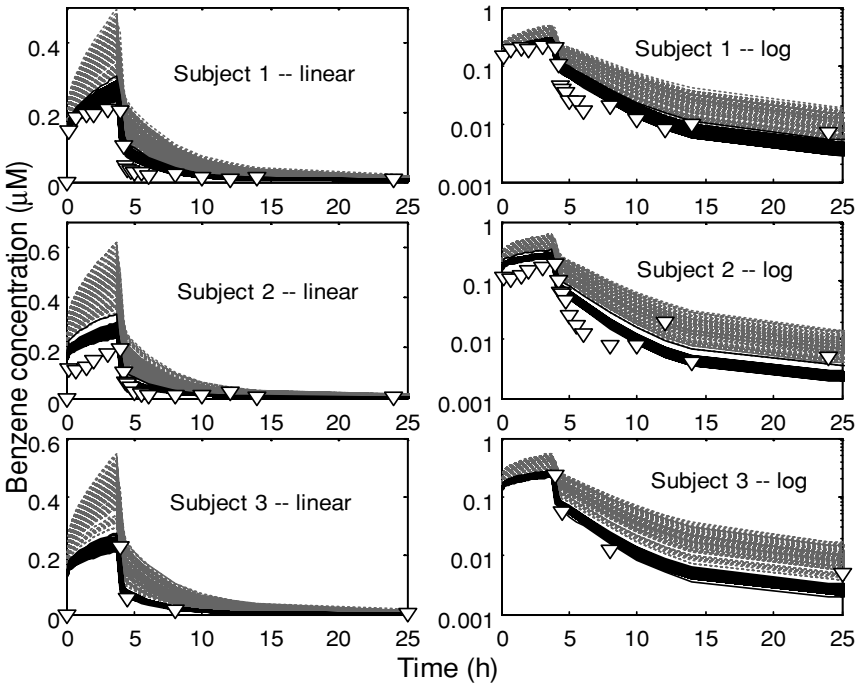

Fig. 2. Model posterior distributions versus data for benzene in exhaled air at higher exposure levels. Data (symbols) are from Pekari *et al.*;[12] black dots are simulations with parameters drawn from individual distributions; gray dots are simulations with parameters drawn from overall population distributions.

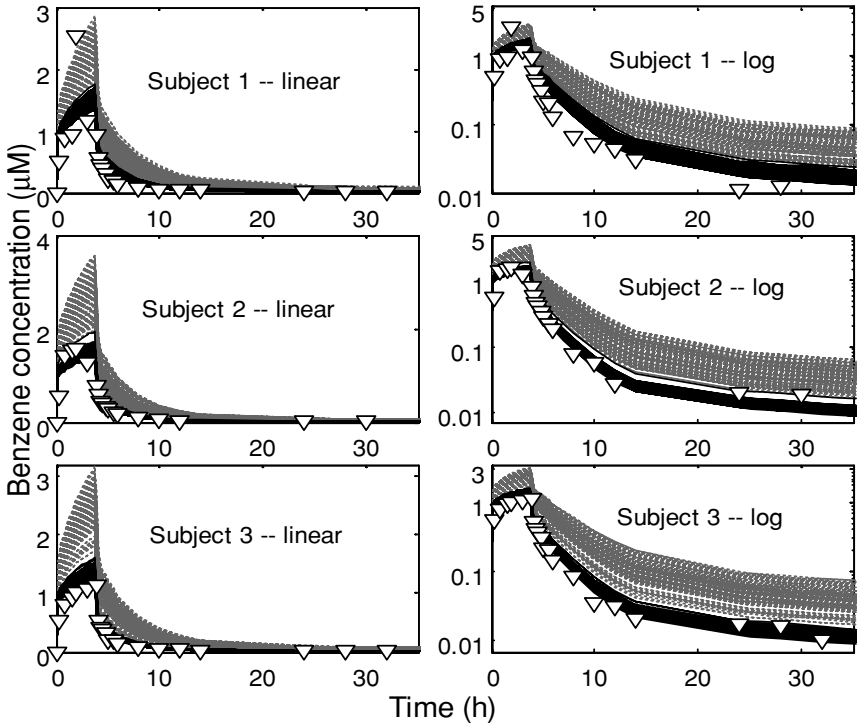

Fig. 3. Model posterior distributions versus data for benzene in blood at higher exposure levels. (See Fig. 2 legend.)

different urinary metabolites and benzene blood and exhaled air concentrations evaluated for sensitivity. Hence, each column specifies the parameter that was varied, and the row indicates the state variable or metric for the respective sensitivity. The covariance matrix for the population is contained in Table VI. The covariance matrices for the three individuals from Pekari *et al.*[12] are contained in Tables VII–IX.

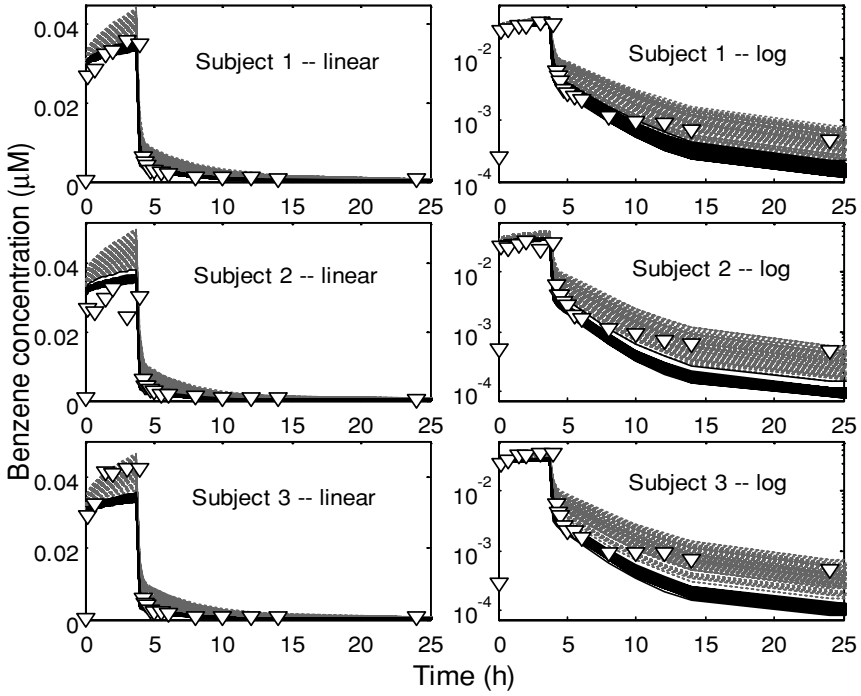

Fig. 4. Model posterior distributions versus data for benzene in exhaled air at lower exposure levels. (See Fig. 2 legend.)

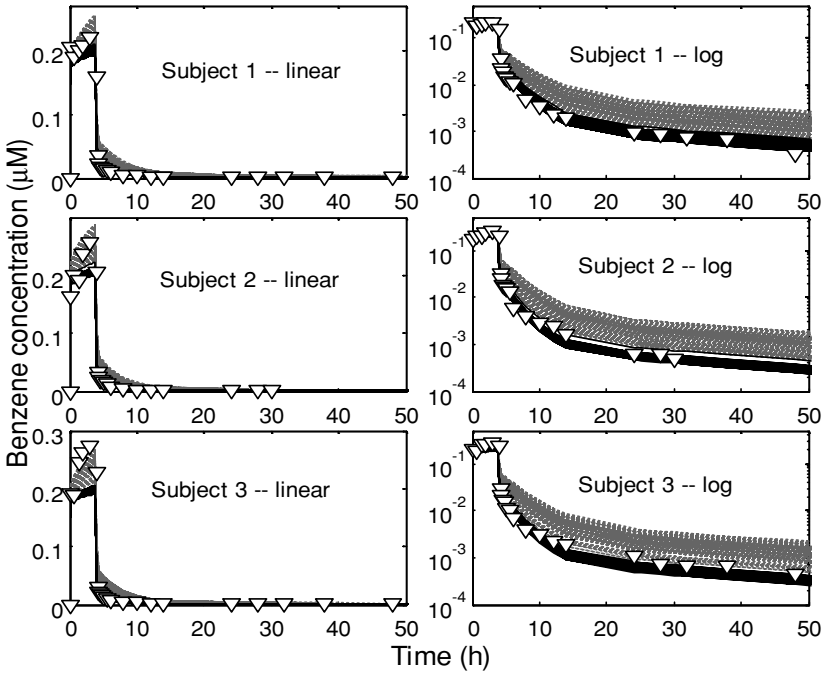

Fig. 5. Model posterior distributions versus data for benzene in blood at lower exposure levels. (See Fig. 2 legend.)

4. DISCUSSION

The model predicted human metabolite data well for MA, PMA, and phenol and hydroquinone conjugates; but the model greatly underpredicted the concentrations of catechol and trihydroxy benzene for the workplace data.[20,21] Since Bayesian methods depend greatly on the accuracy of prior information, small errors in the data used to estimate the priors could account for the need to alter the *MCSim* output for a better fit graphically. The model seems to predict well the exhaled concentration of benzene

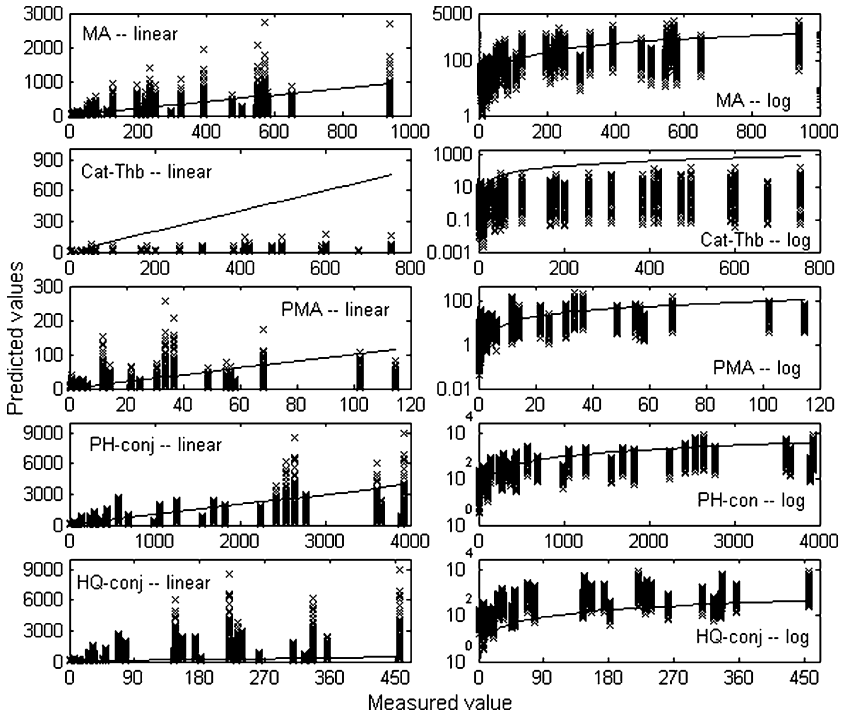

Fig. 6. Model posterior distributions versus metabolite data of Waidyanatha *et al*.[21] Model simulations (×) show the distribution of model predictions in the *y*-dimension plotted against the corresponding measured value on the *x*-axis. The solid line (curve) is $y = x$. The urinary metabolites or metabolite groups are: muconic acid (MA), catechol and trihydroxy benzene (Cat-Thb), phenol and phenol conjugates (PH), phenylmercapturic acid (PMA), and hydroquinone and hydroquinone conjugates (HQ).

Table V. Sensitivity Coefficients for Investigated Parameters

State Variable or Metric	Parameter					
	k_3	k_4	V_{2E1}	V_{PH1}	V_{PH2}	V_{HQ}
MA	0.41	1.31	2.56	0.30	0.025	9.3×10^{-5}
Cat–THB	0.25	0.21	1.88	0.32	0.027	0.022
PMA	1.28	0.24	2.02	0.25	0.020	7.4×10^{-5}
PH	0.097	0.56	2.15	0.33	0.019	1.4×10^{-4}
HQ	0.071	0.15	1.58	0.17	0.014	0.59
$C_{Bl}^{PH} \times C_{Bl}^{HQ}$	0.026	0.27	2.00	0.24	0.020	0.40
C_E^{BZ} (high)	0.12	1.26	5.80	0.32	0.026	3.8×10^{-5}
C_E^{BZ} (low)	0.017	0.14	3.17	0.017	0.0014	1.3×10^{-4}
$CA^{BZ} + CV^{BZ}$ (high)	0.12	1.26	5.80	0.32	0.026	3.8×10^{-5}
$CA^{BZ} + CV^{BZ}$ (low)	0.017	0.14	3.17	0.017	0.0014	1.3×10^{-4}

Note: Values are normalized sensitivity coefficients showing the change in the state variables or metrics indicated in the first column when varying the parameter indicated at the top of each value column.

and the concentration of benzene in blood from Pekari *et al.*,[12] with greater variation in the predictions based on the posterior population distributions as compared to the model solutions using the individual parameter distributions. Since the two studies probably varied in participant physical activity, further experiments focusing on activity levels might further improve the accuracy of the model.

The sensitivity analysis results in Table V indicate that small changes in k_3 only significantly affect the model's prediction of urinary PMA and to a lesser extent MA, while small changes in k_4 only significantly affect the model's predictions of urinary MA, concentrations of benzene in blood and exhaled air (for higher concentrations), and to a lesser extent urinary phenol (PH). The sensitivity of urinary MA and PMA metabolites to changes in k_3 and k_4 is expected based on the roles of these two investigated parameters (the rate constants for conversion of benzene oxide to PMA and MA, respectively). Urinary PH is sensitive to these parameters because the pathways to MA and PMA compete with the pathway to PH. All investigated states show some sensitivity to changes in V_{2E1}, which is also expected considering the frequency of this parameter in the model. The model shows little change in prediction for all considered output variables in response to small variation in the remaining three investigated parameters, V_{PH1}, V_{PH2}, and V_{HQ}, although V_{PH1} has a modest effect on all downstream metabolites and there is reasonable sensitivity of urinary hydroquinone to V_{PH1}.

When the model prediction of one output variable is less sensitive to the change in a particular parameter, the *MCSim* program is more influenced by the data of other output variables (that do show greater sensitivity) when finding the posterior distribution of that particular parameter. Hence k_3, V_{HQ}, and to a lesser extent V_{PH1} and V_{PH2} are more strongly influenced by the occupational urinary data than by the benzene blood and exhaled air data. The distributions for V_{2E1} and k_4 are sensitive to both the urinary metabolite and benzene blood/air data, though the blood/air data have greater influence over

	k_3	k_4	V_{2E1}	V_{PH1}	V_{PH2}	V_{HQ}
k_3	0.0061	−0.012	-3.3×10^{-6}	1.7×10^{-5}	-9.6×10^{-4}	-1.9×10^{-5}
k_4		2.8	2.7×10^{-5}	0.0016	-4.2×10^{-3}	−0.015
V_{2E1}			3.9×10^{-7}	5.6×10^{-8}	9.3×10^{-6}	4.1×10^{-6}
V_{PH1}				1.2×10^{-4}	1.2×10^{-4}	5.5×10^{-5}
V_{PH2}					0.015	-4.7×10^{-4}
V_{HQ}						0.010

Table VI. Covariance Matrix (Log-Space) for Population Posterior Mean Values

	k_3	k_4	V_{2E1}	V_{PH1}	V_{PH2}	V_{HQ}
k_3	0.023	−0.032	1.1×10^{-5}	8.0×10^{-5}	−0.0015	0.019
k_4		8.0	3.2×10^{-4}	−0.0044	−0.080	−0.012
V_{2E1}			1.6×10^{-4}	2.8×10^{-5}	-3.9×10^{-4}	0.0011
V_{PH1}				0.0032	-4.4×10^{-4}	5.1×10^{-4}
V_{PH2}					0.23	0.0044
V_{HQ}						2.0

Table VII. Covariance Matrix (Log-Space) for Posterior Values for the First Individual from Pekari *et al.*[12]

Table VIII. Covariance Matrix (Log-Space) for Posterior Values for the Second Individual from Pekari *et al.*[12]

	k_3	k_4	V_{2E1}	V_{PH1}	V_{PH2}	V_{HQ}
k_3	0.022	−0.046	-3.7×10^{-4}	2.9×10^{-4}	−0.010	−0.0030
k_4		8.2	0.020	−0.013	−0.19	0.20
V_{2E1}			0.0086	-2.5×10^{-4}	0.0036	−0.0012
V_{PH1}				0.0022	0.0020	-7.6×10^{-4}
V_{PH2}					0.41	0.0098
V_{HQ}						1.14

Table IX. Covariance Matrix (Log-Space) for Posterior Values for the Third Individual from Pekari *et al.*[12]

	k_3	k_4	V_{2E1}	V_{PH1}	V_{PH2}	V_{HQ}
k_3	0.024	−0.011	-4.0×10^{-4}	2.7×10^{-4}	−0.0018	−0.0030
k_4		9.8	−0.0038	0.0054	−0.014	0.27
V_{2E1}			0.0046	-1.1×10^{-5}	0.0050	−0.0057
V_{PH1}				0.0014	2.5×10^{-5}	−0.0057
V_{PH2}					0.26	−0.031
V_{HQ}						1.81

V_{2E1} than the metabolite data. Although the data used in the MCMC analysis likely inform the distributions for V_{PH1} and V_{HQ} and none of the data has significant influence over V_{PH2}, the distributions for k_3, k_4, and V_{2E1} can be considered much more accurately determined. The sensitivity of the model output of the product of hydroquinone and phenol blood concentrations was included in the analysis since that particular variable is a potential measure of toxicity. The product of these blood concentrations is clearly most sensitive to V_{2E1}, though it is also influenced by V_{HQ}, k_4, and V_{PH1}. Hence, the accuracy of V_{2E1} is critical to risk assessment, and the posterior distribution for V_{2E1} in Table III seems well determined considering the amount of data used in determining V_{2E1}, including the data used in the simulations[12,20,21] as well as the data used in determining its prior.[18] Using a variety of types of data should aid in better estimates of parameter distributions, but understanding that certain data sets are more critical than others in the determination of each model parameter is also critical in developing the most accurate model.

The off-diagonal covariance matrix values all seem reasonably small for the population and for the three individuals. The variances (on the diagonal) are small except for k_4, but small variances seem logical for the population matrix because that matrix was computed based on iteration outputs for the mean. Since the covariance values are all small, all the investigated parameters appear to be uncorrelated.

From a statistical viewpoint, when both the mathematical model and the statistical model are fully specified at all levels, the approach is referred to as parametric. In the PBPK model, the approach is considered parametric when assuming a distribution form (e.g., log-normal) for how well we know each individual's parameters and a distribution form for the set of parameters from all individuals. A parametric approach is often used when the general form of the distribution in the problem is known. Second, a statistical model is considered to be structured when the variables (distributions) are associated with specific underlying quantities, which occurs naturally with PBPK model. A parametric approach provides an efficient way for estimating the parameters of a PBPK model since it takes full advantage of the distribution structure.

A variety of statistical tools are available for fitting the mathematical models to data with structured variability. Model-fitting tools that do not incorporate prior information on parameter distributions, referred to as "frequentist," include maximum likelihood methods such as nonlinear least squares.[24] The error structure in the data (how sources of error or variability are assigned) can be accommodated by modifying standard techniques to incorporate ideas from repeated measures and cross-over experimental designs. Alternatively, Bayesian statistical models provide a natural framework for analyzing models with hierarchical error structures.[25] One Bayesian technique that has been embraced by a great many applied statisticians in all fields of research is the MCMC method.[26] MCMC methods explore the joint posterior distribution of interest (i.e., the distribution of

all parameters, given that the distributions may not be independent) by providing a mechanism whereby a set of realizations or samples from that distribution can be generated. This set is obtained by carrying out Monte Carlo simulations from a Markov chain constructed so that its stationary distribution is the relevant posterior. Various methodologies exist to carry out the required simulations, including the Gibbs sampling algorithm and the Metropolis-Hastings algorithm. Because of the increasing complexities of statistical models encountered in practice, MCMC provides a much-needed unifying framework within which many complex problems can be analyzed.

Both Bayesians and frequentists need to integrate over possibly high-dimensional probability distributions, such as unknown parameters, to make inferences for the parameter of interest or to make predictions. This basic need motivates the use of MCMC methodology in statistical modeling and inference, since the integration is achieved much more simply and directly via MCMC (albeit, with significant computational time). The past several years have witnessed an explosive growth of interest in MCMC methodology from researchers in almost all areas of statistics and biology. In particular, Bayesian population methods have made some significant contributions in the field of PBPK modeling. In Bois *et al.*,[27] Bayesian statistical inference and physiological modeling were brought together to model the distribution and metabolism of benzene in humans. This approach of combining PBPK models and MCMC methodology for Bayesian inference has been extended to other chemicals such as toluene and styrene.[15,28] The inclusion of the variability predicted by these approaches into risk assessments is expected to be an improvement over previous use of empirical uncertainty factors (e.g., Lipscomb *et al.*[29]).

Bois *et al.*[27] also applied Bayesian analysis to a PBPK model of benzene in humans, using the data of Pekari *et al.*,[12] which are also included in our analysis. The article of Bois and co-workers was one of the first to demonstrate the application of Bayesian analysis to PBPK modeling and its use in predicting population variability, a significant advancement in the potential for mechanistic dosimetry modeling in risk analysis. However, the model used by Bois *et al*. included only a very simple description of benzene metabolites, with the assumption that phenolic metabolites are a fixed fraction of those metabolites. That model does not allow for prediction of target tissue concentrations of phenol itself (as opposed to phenol conjugates), nor of hydroquinone or benzene oxide, both of which are included in our model. Hydroquinone and phenol have been shown to strongly synergize in the induction of genotoxicity *in vivo,*[30] and hydroquinone was shown to strongly enhance colony formation of murine bone marrow cells *in vitro.*[31] Benzene oxide has been shown to be tumorigenic in mice[32] and benzene exposure-related increases in benzene oxide-albumin adducts demonstrated in humans.[33,34] Thus, we believe the current model builds on and is a considerable advancement of the innovative work by Bois and colleagues in that it predicts tissue levels of phenol, hydroquinone, and benzene oxide, all of which are likely contributors to the leukemogenic effects of benzene. Further, the current results are based on data from a much larger number of individuals than that used in the previous analysis, providing for more robust and representative posterior distributions.

A known source of variability that has been better accounted for elsewhere is the effect of activity level on circulation and respiration.[15,35] Not only were we faced with a lack of data on activity level among the subjects in the studies included here, but we were also working with many more metabolic parameters for which the priors are not strongly informative. However, the hypothesis that the effect of known or estimated variability in these metabolic parameters could more than cover the observed variability in the data seemed possible. Therefore, we decided to test the hypothesis that the observed variability in the data would be accounted for by incorporating distributions for *only* the metabolic parameters by fixing the values of most physiological variables to standard values used in PBPK modeling (e.g., Brown *et al.*[16]) and the measured partition coefficients to those measured or estimated elsewhere.

Incorporation of dependence on activity level and variability and uncertainty in physiological parameters and partition coefficients would almost certainly have resulted in much closer correlations between predictions and the data and should probably be added before the benzene PBPK model is used in a human risk assessment, but we believe there is scientific value in first testing this more stringent assumption presented here. While we do not know precise activity levels for the individuals whose data are being simulated here, Jonsson and Johanson[28] found the best description of their data for toluene when "the increased perfusion of perirenal fat was set to a constant level during all exercise levels," which indicates

that categorical assignment of values based on general activity patterns (e.g., resting, some movement, light work) is sufficient.

At the beginning of this study, additional data were considered from Berlin *et al*.,[36] who measured benzene concentrations in exhaled breath after inhalation exposures. Results reported by Berlin *et al*. were different enough from those of Pekari *et al.*[12] that including both sets of data in our analysis became problematic. Since the Pekari *et al*. data seemed more informative, our attempt to include the Berlin data was abandoned. In early studies incorporating the Berlin data, the model fits of benzene concentration in blood and exhaled air to the data of Pekari data were fairly good and appeared to be without significant bias. At least in those cases, the model predicted the relationship between blood concentrations and exhaled air concentrations. Recognizing that the Berlin *et al.*[36] and Waidyanatha *et al.*[21] data sets are from distinct populations, we note that there is a tendency for the model to overpredict both the amount in exhaled breath and urinary excretion when the Berlin data are incorporated into the study. Since any benzene inhaled must be excreted by one of these routes or bind to tissue macromolecules (first-order rates from phenol and hydroquinone), the only way to decrease both exhaled breath predictions *and* urinary excretion predictions would be to increase the amount predicted as binding to macromolecules or decrease the predicted inhalation rate. Since we believe the rate constants for binding to macromolecules represent nonenzymatic reactions that should be independent of species, their values were not updated from those estimated by Cole *et al.*[9,10] using mouse *in vivo* data.

Thus, we could potentially correct the overprediction of the Berlin *et al.*[36] and Waidyanatha *et al.*[21] data by updating k_9 and k_{10}. If we had allowed those parameters to be updated, better fits probably could have been obtained without further insight. Instead, the failure of the model to fit the data given the constraints of holding those parameters constants led us to the possibility that we had overpredicted the rate of uptake by inhalation. Benzene has a blood:air partition coefficient of 7.8.[37] While this is relatively low and benzene has low aqueous solubility, one might expect a limited wash-in/wash-out effect that would lower absorption from the amount predicted by the classic venous ventilation model used here (see Gerde & Dahl[38]). After this analysis, we decided not to use the data from Berlin *et al*. in our study rather than alter k_9 or k_{10} or the blood:air partition coefficient. After the decision to exclude the data of Berlin *et al*. from our analysis, k_9 and k_{10} were investigated briefly through the MCMC method using priors based on values from Cole *et al.*[9,10] The intention was to improve the results with catechol and trihydroxy benzene, but no significant improvement resulted in the fit to data from either Pekari *et al.*[12] or the occupational data from Rothman *et al*.[20] and Waidyanatha *et al.*[21].

The difference between a model adjustment by increasing the macromolecule binding constants and decreasing predicted inhalation rates is potentially significant because the latter would result in a reduction in the prediction of total phenol and hydroquinone production and hence in potential target tissue dosimetry of active metabolites. Future work on benzene PBPK modeling for humans should probably first seek to implement a more anatomically accurate inhalation model, such as those described by Sarangapani *et al.*[39] or Csanády *et al.*[40] before updating the macromolecule binding constants. If the predicted pharmacokinetic distributions still do not cover the data after making such structural changes to eliminate model bias, we would then have greater support for including other sources of variability and possibly updating their distributions as well.

Given the constraints of fixing many model parameters to standard or previously reported values, the fact that the model does a fairly good job of describing the data from two different studies suggests that the model structure is essentially sound and affirms the use of key parameters from *in vitro* or laboratory animal studies. The significant difference between the prior and posterior distributions for V_{2E1} and V_{PH2} shows that uncertainty may remain in the extrapolation of a PBPK model to humans even with prior data such as we had for benzene. The model predicts variability well after allowing for variation in only a few metabolic parameters, affirming our hypothesis that only a few distributional parameters are necessary. Fewer than six distributional parameters may be sufficient as well, but we have shown how variation in many parameters may be unnecessary. The covariance analysis suggests that no pair of investigated parameters is correlated, but whether the variation produced by different parameters overlaps is uncertain. Fortunately, we have a number of human data for benzene to use in parameter estimation and demonstrate model quality. However, these results may guide similar *in vitro* to *in vivo* and animal-to-human extrapolations through PBPK modeling for other compounds with fewer or no human data available.

ACKNOWLEDGMENTS

The authors would like to thank Dr. Rory Conolly, Dr. Melvin Andersen, Dr. Woody Setzer, and Dr. Cammey Cole for helpful discussions during the development of this article and Dr. Barbara Kuyper for editorial assistance. Research support for Karen Yokley and Paul Schlosser was provided by member companies of the American Chemistry Council through the Long-Range Research Initiative and a subsequent unrestricted grant to North Carolina State University from CIIT. Additional research support for Karen Yokley and Hien Tran was provided by the Joint DMS/NIGMS Initiative to Support Research in the Area of Mathematical Biology under Grant 1R01GM67299-01. This research was also supported in part by grants from the National Institute of Environmental Health Sciences (P30ES10126 and P42ES05948) and by the intramural research program of National Institutes of Health, National Cancer Institute.

APPENDIX 1: MODEL SYMBOLS

The following symbols and abbreviations are used in the PBPK model given in Appendix 2. Units of the symbols are given in parentheses.

Chemical Abbreviations

BZ	Benzene
BO	Benzene oxide
PH	Phenol
HQ	Hydroquinone
MA	Muconic acid
PMA	Phenylmercapturic acid
PH-Conj	Phenol conjugates
HQ-Conj	Hydroquinone conjugates
Cat	Catechol
THB	Trihydroxy benzene

Compartment Abbreviations

F	Fat
S	Slowly or poorly perfused tissue
R	Rapidly or richly perfused tissue
K	Kidney
*L*1	Zone 1 of the liver
*L*2	Zone 2 of the liver
*L*3	Zone 3 of the liver
Bl	Blood
Stom	Stomach
I	Inhaled air
E	Exhaled air

Primary Symbols

C_i^j	Concentration of chemical i in tissue j (μmol/L)
CA^{BZ}	Concentration of BZ in the arterial blood (μmol/L)
CV^{BZ}	Concentration of BZ in the venous blood (μmol/L)
CV_j^i	Concentration of chemical i in venous blood from tissue j (μmol/L)
C_I^{BZ}	Concentration of BZ in inhaled air (μmol/L)
C_E^{BZ}	Concentration of BZ in exhaled air (μmol/L)
AM^i	Amount of chemical i in urine (μmol)
AM^{Stom}	Amount of BZ in the stomach (μmol)
RM_j^i	Rate of metabolism of chemical i to chemical j (μmol/hour)
Q_j	Flow in tissue j (L/hour)
Q_{AvV}	Alveolar ventilation (L/hour)
Q_{card}	Cardiac blood output (L/hour)
P_j^i	Tissue j/blood partition coefficient for chemical i
$P_{Bl:Air}^{BZ}$	Blood/air partition coefficient for BZ
BW	Body weight (kg)
V_j	Volume of tissue j (L)
T_L	Total mass of the liver (g)
C^{MP}	Concentration of microsomal protein per gram of tissue in the liver (mg/g)
C^{CP}	Concentration of cytosolic protein per gram of tissue in the liver (mg/g)
V_{2E1}	CYP2E1 specific activity as determined by the oxidation of p-nitrophenol to p-nitrocatechol (μmol/mg/hour)
A^i	Affinity parameter for CYP2E1 for substrate i (L/μmol)
k_1, k_5–k_7	Efficiencies of CYP2E1 for specific oxidation relative to V_{2E1} (L/μmol)
k_2–k_4	First-order rates of metabolism (1/hour)
k_8	Rate of uptake from the stomach to the liver (1/hour)
k_9, k_{10}	Binding coefficients (1/hour)
V_{PH1}, V_{PH2}	Maximum rates of metabolism of PH by two sulfate transferases (μmol/mg/hour)
$K_{m,1}^{PH}$, $K_{m,2}^{PH}$	Concentrations at half-saturation of PH by two sulfate transferases (μmol/L)
V_{HQ}	Maximum rate of metabolism for HQ (μmol/mg/hour)

K_m^{HQ} Concentration at half-saturation for HQ (μmol/L)
k_{Card} Proportionality constant between BW and Q_{Card} (L/(hour × kg))
k_{QAvV} Proportionality constant between Q_{Card} and Q_{AvV} (unit-less)
f_{alv} Fraction of each inhaled breath that perfuses the alveolar space (unit-less)

APPENDIX 2: MATHEMATICAL MODEL

The following system of ordinary differential equations that was derived in Cole *et al.*[9,10] was based on a perfusion-limited model, or equivalently, a flow-limited model of disposition. More specifically, the rate of uptake of benzene into a tissue compartment was assumed to be limited by the blood flow rate to the tissue rather than the rate of diffusion across the cell membrane. For the sake of completeness, the model equations and the differential equations (grouped by chemical) are given below.

Explicit Equations

Concentration of chemical i in venous blood leaving compartment j: $CV_j^i = \frac{C_j^i}{P_j^i}$

Cardiac flow: $Q_{card} = Q_F + Q_S + Q_R + Q_L + Q_K$

Concentration of BZ in venous blood:

$$CV^{BZ} = \frac{CV_F^{BZ} Q_F + CV_S^{BZ} Q_S + CV_R^{BZ} Q_R + CV_L^{BZ} Q_L + CV_K^{BZ} Q_K}{Q_{Card}}$$

Concentration of BZ in arterial blood:

$$CA^{BZ} = \frac{Q_{AvV} C_I^{BZ} + Q_{Card} CV^{BZ}}{\frac{Q_{AvV}}{P_{Bl:Air}} + Q_{Card}}$$

CYP2E1 activity in the liver:

$$RM_{BO,L3}^{BZ} = k_1 \frac{V_{2E1} C_{L3}^{BZ}}{D_L} C^{MP} \frac{T_L}{3}$$

$$RM_{HQ,L3}^{PH} = k_5 \frac{V_{2E1} C_{L3}^{PH}}{D_L} C^{MP} \frac{T_L}{3}$$

$$RM_{Cat,L3}^{PH} = k_6 \frac{V_{2E1} C_{L3}^{PH}}{D_L} C^{MP} \frac{T_L}{3}$$

$$RM_{THB,L3}^{HQ} = k_7 \frac{V_{2E1} C_{L3}^{HQ}}{D_L} C^{MP} \frac{T_L}{3}$$

$$D_L = 1 + A^{BZ} C_{L3}^{BZ} + A^{PH} C_{L3}^{PH} + A^{HQ} C_{L3}^{HQ}$$

CYP2E1 activity in the kidney:

$$RM_{BO,K}^{BZ} = k_1 \frac{V_{2E1}}{10} \frac{C_K^{BZ}}{D_K} C^{MP} T_K$$

$$RM_{HQ,K}^{PH} = k_5 \frac{V_{2E1}}{10} \frac{C_K^{PH}}{D_K} C^{MP} T_K$$

$$RM_{Cat,K}^{PH} = k_6 \frac{V_{2E1}}{10} \frac{C_K^{PH}}{D_K} C^{MP} T_K$$

$$RM_{THB,K}^{HQ} = k_7 \frac{V_{2E1}}{10} \frac{C_K^{HQ}}{D_K} C^{MP} T_K$$

$$D_K = 1 + A^{BZ} C_K^{BZ} + A^{PH} C_K^{PH} + A^{HQ} C_K^{HQ}$$

Total mass of j = liver or kidney: $T_j = V_j \cdot 10^3$g/L

Metabolism of BO to PH in compartment j: $RM_{PH,j}^{BO} = k_2 \, C_j^{BO} V_j$

Metabolism of BO to PMA in compartment j: $RM_{PMA,j}^{BO} = k_3 \, C_j^{BO} V_j$

Metabolism of BO to MA in compartment j: $RM_{MA,L3}^{BO} = k_4 C_{L3}^{BO} \frac{V_L}{3}$

Conjugation of PH:

$$RM_{Conj,L1}^{PH} = \left(\frac{V_{PH1} C_{L1}^{PH}}{K_{m,1}^{PH} + C_{L1}^{PH}} + \frac{V_{PH2} C_{L1}^{PH}}{K_{m,2}^{PH} + C_{L1}^{PH}} \right) C^{CP} \frac{T_L}{3}$$

Conjugation of HQ:

$$RM_{Conj,L3}^{HQ} = \frac{V_{HQ} C_{L3}^{HQ}}{K_m^{HQ} + C_{L3}^{HQ}} C^{MP} \frac{T_L}{3}$$

Concentration of exhaled benzene:

$$C_E^{BZ} = (1 - f_{alv}) \cdot C_I^{BZ} + f_{alv} \left[Q_{Card} \cdot (CV^{BZ} - CA^{BZ}) + Q_{AvV} \cdot C_I^{BZ} \right] / Q_{AvV}$$

Benzene

Fat:

$$V_F \frac{dC_F^{BZ}}{dt} = Q_F \left(CA^{BZ} - CV_F^{BZ} \right)$$

Slowly:

$$V_S \frac{dC_S^{BZ}}{dt} = Q_S \left(CA^{BZ} - CV_S^{BZ} \right)$$

Rapidly:

$$V_R \frac{dC_R^{BZ}}{dt} = Q_R \left(CA^{BZ} - CV_R^{BZ} \right)$$

Kidney:

$$V_K \frac{dC_K^{BZ}}{dt} = Q_K \left(CA^{BZ} - CV_K^{BZ} \right) - RM_{BO,K}^{BZ}$$

Liver (Zone 1):

$$\frac{V_L}{3}\frac{dC_{L1}^{BZ}}{dt} = Q_L\left(CA^{BZ} - C_{L1}^{BZ}\right) + k_8 AM^{Stom}$$

Liver (Zone 2):

$$\frac{V_L}{3}\frac{dC_{L2}^{BZ}}{dt} = Q_L\left(C_{L1}^{BZ} - C_{L2}^{BZ}\right)$$

Liver (Zone 3):

$$\frac{V_L}{3}\frac{dC_{L3}^{BZ}}{dt} = Q_L\left(C_{L2}^{BZ} - CV_{L3}^{BZ}\right) - RM_{BO,L3}^{BZ}$$

Stomach: $dAM^{Stom}/dt = -k_8 \cdot AM^{Stom}$

Amount Exhaled:

$$\frac{dAM_E^{BZ}}{dt} = Q_{Card}(CV^{BZ} - CA^{BZ}) + Q_{AvV} \cdot C_I^{BZ}$$

Benzene Oxide

Blood:

$$V_{Bl}\frac{dC_{Bl}^{BO}}{dt} = Q_F CV_F^{BO} + Q_S CV_S^{BO} + Q_R CV_R^{BO} + Q_K CV_K^{BO} + Q_L CV_{L3}^{BO} - Q_{Card} C_{Bl}^{BO} - RM_{PMA,Bl}^{BO} - RM_{PH,Bl}^{BO}$$

Fat:

$$V_F\frac{dC_F^{BO}}{dt} = Q_F\left(C_{Bl}^{BO} - CV_F^{BO}\right) - RM_{PMA,F}^{BO} - RM_{PH,F}^{BO}$$

Slowly:

$$V_S\frac{dC_S^{BO}}{dt} = Q_S\left(C_{Bl}^{BO} - CV_S^{BO}\right) - RM_{PMA,S}^{BO} - RM_{PH,S}^{BO}$$

Rapidly:

$$V_R\frac{dC_R^{BO}}{dt} = Q_R\left(C_{Bl}^{BO} - CV_R^{BO}\right) - RM_{PMA,R}^{BO} - RM_{PH,R}^{BO}$$

Kidney:

$$V_K\frac{dC_K^{BO}}{dt} = Q_K\left(C_{Bl}^{BO} - CV_K^{BO}\right) + RM_{BO,K}^{BZ} - RM_{PH,K}^{BO} - RM_{PMA,K}^{BO}$$

Liver(Zone 1):

$$\frac{V_L}{3}\frac{dC_{L1}^{BO}}{dt} = Q_L\left(C_{Bl}^{BO} - C_{L1}^{BO}\right) - RM_{PH,L1}^{BO}$$

Liver (Zone 2):

$$\frac{V_L}{3}\frac{dC_{L2}^{BO}}{dt} = Q_L\left(C_{L1}^{BO} - C_{L2}^{BO}\right) - RM_{PH,L2}^{BO}$$

Liver (Zone 3):

$$\frac{V_L}{3}\frac{dC_{L3}^{BO}}{dt} = Q_L\left(C_{L2}^{BO} - CV_{L3}^{BO}\right) + RM_{BO,L3}^{BZ} - RM_{PH,L3}^{BO} - RM_{MA,L3}^{BO} - RM_{PMA,L3}^{BO}$$

Muconic Acid

$$\frac{dAM^{MA}}{dt} = RM_{MA,L3}^{BO}$$

Phenylmercapturic Acid

$$\frac{dAM^{PMA}}{dt} = RM_{PMA,Bl}^{BO} + RM_{PMA,F}^{BO} + RM_{PMA,S}^{BO} + RM_{PMA,R}^{BO} + RM_{PMA,K}^{BO} + RM_{PMA,L3}^{BO}$$

Phenol

Blood:

$$V_{Bl}\frac{dC_{Bl}^{PH}}{dt} = Q_F CV_F^{PH} + Q_S CV_S^{PH} + Q_R CV_R^{PH} + Q_K CV_K^{PH} + Q_L CV_{L3}^{PH} - Q_{Card} C_{Bl}^{PH} + RM_{PH,Bl}^{BO} - k_9 C_{Bl}^{PH} V_{Bl}$$

Fat:

$$V_F\frac{dC_F^{PH}}{dt} = Q_F\left(C_{Bl}^{PH} - CV_F^{PH}\right) + RM_{PH,F}^{BO} - k_9 C_F^{PH} V_F$$

Slowly:

$$V_S\frac{dC_S^{PH}}{dt} = Q_S\left(C_{Bl}^{PH} - CV_S^{PH}\right) + RM_{PH,S}^{BO} - k_9 C_S^{PH} V_S$$

Rapidly:

$$V_R\frac{dC_R^{PH}}{dt} = Q_R\left(C_{Bl}^{PH} - CV_R^{PH}\right) + RM_{PH,R}^{BO} - k_9 C_R^{PH} V_R$$

Kidney:

$$V_K \frac{dC_K^{PH}}{dt} = Q_K\left(C_{Bl}^{PH} - CV_K^{PH}\right) + RM_{PH,K}^{BO} - RM_{HQ,K}^{PH} - RM_{Cat,K}^{PH} - k_9 C_K^{PH} V_K$$

Liver (Zone 1):

$$\frac{V_L}{3}\frac{dC_{L1}^{PH}}{dt} = Q_L\left(C_{Bl}^{PH} - C_{L1}^{PH}\right) + RM_{PH,L1}^{BO} - RM_{Conj,L1}^{PH} - k_9 C_{L1}^{PH}\frac{V_L}{3}$$

Liver (Zone 2):

$$\frac{V_L}{3}\frac{dC_{L2}^{PH}}{dt} = Q_L\left(C_{L1}^{PH} - C_{L2}^{PH}\right) + RM_{PH,L2}^{BO} - k_9 C_{L2}^{PH}\frac{V_L}{3}$$

Liver (Zone 3):

$$\frac{V_L}{3}\frac{dC_{L3}^{PH}}{dt} = Q_L\left(C_{L2}^{PH} - CV_{L3}^{PH}\right) + RM_{PH,L3}^{BO} - RM_{HQ,L3}^{PH} - RM_{Cat,L3}^{PH} - k_9 C_{L3}^{PH}\frac{V_L}{3}$$

Phenol Conjugates

$$\frac{dAM^{PH-Conj}}{dt} = RM_{Conj,L1}^{PH}$$

Hydroquinone

Blood:

$$V_{Bl}\frac{dC_{Bl}^{HQ}}{dt} = Q_F CV_F^{HQ} + Q_S CV_S^{HQ} + Q_R CV_R^{HQ} + Q_K CV_K^{HQ} + Q_L CV_{L3}^{HQ} - Q_{Card} C_{Bl}^{HQ} - k_{10} C_{Bl}^{HQ} V_{Bl}$$

Fat:

$$V_F\frac{dC_F^{HQ}}{dt} = Q_F\left(C_{Bl}^{HQ} - CV_F^{HQ}\right) - k_{10} C_F^{HQ} V_F$$

Slowly:

$$V_S\frac{dC_S^{HQ}}{dt} = Q_S\left(C_{Bl}^{HQ} - CV_S^{HQ}\right) - k_{10} C_S^{HQ} V_S$$

Rapidly:

$$V_R\frac{dC_R^{HQ}}{dt} = Q_R\left(C_{Bl}^{HQ} - CV_R^{HQ}\right) - k_{10} C_R^{HQ} V_R$$

Kidney:

$$V_K\frac{dC_K^{HQ}}{dt} = Q_K\left(C_{Bl}^{HQ} - CV_K^{HQ}\right) + RM_{HQ,K}^{PH} - RM_{THB,K}^{HQ} - k_{10} C_K^{HQ} V_K$$

Liver (Zone 1):

$$\frac{V_L}{3}\frac{dC_{L1}^{HQ}}{dt} = Q_L\left(C_{Bl}^{HQ} - C_{L1}^{HQ}\right) - k_{10} C_{L1}^{HQ}\frac{V_L}{3}$$

Liver (Zone 2):

$$\frac{V_L}{3}\frac{dC_{L2}^{HQ}}{dt} = Q_L\left(C_{L1}^{HQ} - C_{L2}^{HQ}\right) - k_{10} C_{L2}^{HQ}\frac{V_L}{3}$$

Liver (Zone 3):

$$\frac{V_L}{3}\frac{dC_{L3}^{HQ}}{dt} = Q_L\left(C_{L2}^{HQ} - CV_{L3}^{HQ}\right) + RM_{HQ,L3}^{PH} - RM_{THB,L3}^{HQ} - RM_{Conj,L3}^{HQ} - k_{10} C_{L3}^{HQ}\frac{V_L}{3}$$

Hydroquinone Conjugates

$$\frac{dAM^{HQ-Conj}}{dt} = RM_{Conj,L3}^{HQ}$$

Catechol and Trihydroxy Benzene

$$\frac{dAM^{Cat/THB}}{dt} = RM_{Cat,L3}^{PH} + RM_{Cat,K}^{PH} + RM_{THB,L3}^{HQ} + RM_{THB,K}^{HQ}$$

REFERENCES

1. Runion, H. E., & Scott, L. M. (1985). Benzene exposure in the United States 1978–1983: An overview. *American Journal of Industrial Medicine*, 7(5–6), 385–393.
2. Wallace, L. (1990). Major sources of exposure to benzene and other volatile organic chemicals. *Risk Analysis*, *10*(1), 59–64.
3. Ayres, P. H., Taylor, W. D., & Olson, M. J. (1994). Solvents. In A. W. Hayes (Ed.), *Principles and Methods of Toxicology*, 3rd ed. New York: Raven Press Ltd.
4. Glass, D. C., Gray, C. N., Jolley, D. J., Gibbons, C., Sim, M. R., Fritschi, L., Adams, G. G., Bisby, J. A., & Manuell, R. (2003). Leukemia risk associated with low-level benzene exposure. *Epidemiology*, *14*(5), 569–577.
5. Yardley-Jones, A., Anderson, D., & Parke, D. V. (1991). The toxicity of benzene and its metabolism and molecular pathology in human risk assessment. *British Journal of Industrial Medicine*, *48*(7), 437–444.
6. Haddad, S., Beliveau, M., Tardif, R., & Krishnan, K. (2001). A PBPK modeling-based approach to account for interactions in

the health risk assessment of chemical mixtures. *Toxicological Sciences*, *63*(1), 125–131.
7. Cahill, T. M., Cousins, I., & MacKay, D. (2003). Development and application of a generalized physiologically based pharmacokinetic model for multiple environmental contaminants. *Environmental Toxicology and Chemistry*, *22*(1), 26–34.
8. Cole, C. E., Tran, H. T., & Schlosser, P. M. (2001). Physiologically based pharmacokinetic modeling of benzene metabolism in mice through extrapolation from in vitro to in vivo. *Journal of Toxiciology and Environmental Health, Part A*, *62*(6), 439–465.
9. Cole, C., Schlosser, P. M., & Tran, H. T. (2002). *A Multicompartment Liver-Based Pharmacokinetic Model for Benzene and Its Metabolites in Mice*. Technical Report CRSC-TR02-17, Center for Research in Scientific Computation, North Carolina State University, Raleigh, NC. Available at www.ncsu.edu/crsc/reports/ftp/pdf/crsc-tr02-17.pdf.
10. Cole, C., Schlosser, P. M., & Tran, H. T. (submitted). A multicompartment liver-based pharmacokinetic model for benzene and its metabolites in mice. *Journal of Mathematical Biology*.
11. Bois, F. Y., & Maszle, D. R. (1997). MCSim: A Monte Carlo simulation program. User's guide. *Journal of Statistical Software*, *2*(9). Available at http://bioweb.pasteur.fr/docs/mcsim/MCSim.manual.html.
12. Pekari, K., Vainiotalo, S., Heikkila, P., Palotie, A., Luotamo, M., & Riihimaki, V. (1992). Biological monitoring of occupational exposure to low levels of benzene. *Scandinavian Journal of Work and Environmental Health*, *18*(5), 317–322.
13. Davies, B., & Morris, T. (1993). Physiological parameters in laboratory animals and humans. *Pharmaceutical Research*, *10*(7), 1093–1095.
14. Csanády, G. A., Guengerich, F. P., & Bond, J. A. (1992). Comparison of the biotransformation of 1,3-butadiene and its metabolite, butadiene monoepoxide, by hepatic and pulmonary tissues from humans. *Carcinogenesis*, *13*(7), 1143–1153.
15. Jonsson, F., & Johanson, G. (2002). Physiologically based modeling of the inhalation kinetics of styrene in humans using a Bayesian population approach. *Toxicology and Applied Pharmacology*, *179*(1), 35–49.
16. Brown, R. P., Foran, J., Olin, S., & Robinson, D. (1994). *Physiological Parameter Values for PBPK Models*. Washington, DC: International Life Science Institute (ILSI) Risk Science Institute (RSI). Available at orig.ilsi.org/publications/pubslist.cfm?publicationid=624.
17. Clark, B., & Smith, D. A. (1984). Pharmacokinetics and toxicity testing. *Critical Reviews in Toxicology*, *12*(4), 343–385.
18. Seaton, M. J., Schlosser, P. M., Bond, J. A., & Medinsky, M. A. (1994). Benzene metabolism by human liver microsomes in relation to cytochrome P450 2E1 activity. *Carcinogenesis*, *15*(9), 1799–1806.
19. Seaton, M. J., Schlosser, P. M., & Medinsky, M. A. (1995). *In vitro* conjugation of benzene metabolites by human liver: Potential influence of interindividual variability on benzene toxicity. *Carcinogenesis*, *16*(7), 1519–1527.
20. Rothman, N., Bechtold, W. E., Yin, S. N., Dosemeci, M., Li, G. L., Wang, Y. Z., Griffith, W. C., Smith, M. T., & Hayes, R. B. (1998). Urinary excretion of phenol, catechol, hydroquinone, and muconic acid by workers occupationally exposed to benzene. *Occupational and Environmental Medicine*, *55*(10), 705–711.
21. Waidyanatha, S., Rothman, N., Li, G. L., Smith, M. T., Yin, S. N., & Rappaport, S. M. (2004). Rapid determination of six urinary benzene metabolites in occupationally exposed and unexposed subjects. *Analytical Biochemistry*, *327*(2), 184–199.
22. Schlosser, P. M. (1994). Experimental design for parameter estimation through sensitivity analysis. *Journal of Toxicology and Environmental Health*, *43*(4), 495–530.
23. Geyer, C. J. (1992). Practical Markov chain Monte Carlo. *Statistical Science*, *7*(4), 473–483.
24. Bates, D. M., & Watts, D. G. (1998). *Nonlinear Regression Analysis and Its Applications*. New York: John Wiley & Sons, Inc.
25. Gelman, A., Bois, F., & Jiang, J. (1996). Physiological pharmacokinetic analysis using population modeling and informative prior distributions. *Journal of the American Statistical Association*, *91*(436), 1400–1412.
26. Gilks, W. R., Richardson, S., & Spiegelhalter, D. J. (1996). *Markov Chain Monte Carlo in Practice*. Boca Raton, FL: Chapman & Hall/CRC.
27. Bois, F. Y., Jackson, E. T., Pekari, K., & Smith, M. T. (1996). Population toxicokinetics of benzene. *Environmental Health Perspectives*, *104*(Suppl. 6), 1405–1411.
28. Jonsson, F., & Johanson, G. (2001). Bayesian estimation of variability in adipose tissue blood flow in man by physiologically based pharmacokinetic modeling of inhalation exposure to toluene. *Toxicology*, *157*(3), 177–193.
29. Lipscomb, J. C., Teuschler, L. K., Swartout, J., Popken, D., Cox, T., & Kedderis, G. L. (2003). The impact of cytochrome P450 2E1-dependent metabolic variance on a risk-relevant pharmacokinetic outcome in humans. *Risk Analysis*, *23*(6), 1221–1238.
30. Barale, R., Marrazzini, A., Betti, C., Vangelisti, V., Loprieno, N., & Barrai, I. (1990). Genotoxicity of two metabolites of benzene: Phenol and hydroquinone show strong synergistic effects in vivo. *Mutation Research*, *244*(1), 15–20.
31. Irons, R. D., Stillman, W. S., Colagiovanni, D. B., & Henry, V. A. (1992). Synergistic action of benzene metabolite hydroquinone on myelopoietic stimulating activity of granulocyte/macrophage colony-stimulating in vitro. *Proceedings of the National Academy of Sciences USA*, *89*(9), 3691–3695.
32. Busby, W. F., Jr., Wang, J.-S., Stevens, E. K., Padykula, R. E., Aleksejczyk, R. A., & Berchtold, G. A. (1990). Lung tumorigenicity of benzene oxide, benzene dihydrodiols and benzene diolepoxides in the BLU:Ha newborn mouse assay. *Carcinogenesis*, *11*(9), 1473–1478.
33. Rappaport, S. M., Waidyanatha, S., Qu, Q. S., Shore, R., Jin, X. M., Cohen, B., Chen, L. C., Melikian, A. A., Li, G. L., Yin, S. N., Yan, H. F., Xu, B. H., Mu, R. D., Li, Y. Y., Zhang, X. L., & Li, K. Q. (2002). Albumin adducts of benzene oxide and 1,4-benzoquinone as measures of human benzene metabolism. *Cancer Research*, *62*(5), 1330–1337.
34. Rappaport, S. M., Yeowell-O'Connell, K., Smith, M. T., Dosemeci, M., Hayes, R. B., Zhang, L. P., Li, G. L., Yin, S. N., & Rothman, N. (2002). Non-linear production of benzene oxide-albumin adducts with human exposure to benzene. *Journal of Chromatography B, Analytical Technologies in the Biomedical and Life Sciences*, *778*(1–2), 367–374.
35. Jonsson, F., Bois, F. Y., & Johanson, G. (2001). Assessing the reliability of PBPK models using data from methyl chloride-exposed, non-conjugating human subjects. *Archives of Toxicology*, *75*(4), 189–199.
36. Berlin, M., Gage, J., Gullberg, B., Holm, S., Knutsson, P., Eng, C., & Tunek, A. (1980). Breath concentration as an index of health risk from benzene. *Scandinavian Journal of Work and Environmental Health*, *6*(2), 104–111.
37. Brown, E. A., Shelley, M. L., & Fisher, J. W. (1998). A pharmacokinetic study of occupational and environmental benzene exposure with regard to gender. *Risk Analysis*, *18*(2), 205–213.
38. Gerde, P., & Dahl, A. R. (1991). A model for the uptake of inhaled vapors in the nose of the dog during cyclic breathing. *Toxicology and Applied Pharmacology*, *109*(2), 276–288.
39. Sarangapani, R., Teeguarden, J. G., Cruzan, G., Clewell, H. J., & Andersen, M. E. (2002). Physiologically based

pharmacokinetic modeling of styrene and styrene oxide respiratory-tract dosimetry in rodents and humans. *Inhalation Toxicology*, *14*(8), 789–834.
40. Csanády, G. A., Kessler, W., Hoffmann, H. D., & Filser, J. G. (2003). A toxicokinetic model for styrene and its metabolite styrene-7,8-oxide in mouse, rat and human with special emphasis on the lung. *Toxicology Letters*, *138*(1–2), 75–102.
41. Lovern, M. R., Maris, M. E., & Schlosser, P. M. (1999). Use of a mathematical model of rodent *in vitro* metabolism to predict human in vitro metabolism data. *Carcinogenesis*, *20*(8), 1511–1520.
42. Leung, H.-W., Poland, A., Paustenbach, D. J., Murray, F. J., & Andersen, M. E. (1990). Pharmacokinetics of [125I]-2-iodo-3,7,8-trichlorodibenzo-p-dioxin in mice: Analysis with a physiological modeling approach. *Toxicology and Applied Pharmacology*, *103*(3), 411–419.